

## RESULTS OF SPATIAL STRUCTURE OF ATMOSPHERE RADIATION IN A SPECTRAL RANGE (1.5–2) $\mu\text{m}$ RESEARCH

Anton M. Mishchenko <sup>1\*</sup>, Sergei S. Rachkovsky <sup>2</sup>, Vladimir A. Smolin <sup>2</sup>,  
and Igor V. Yakimenko <sup>2</sup>

<sup>1</sup> *Military Academy of Army Air Defence of Russian Armed Forces of Marshall of the Soviet Union A.M. Vasilevsky (MA AAD of RF AF),*

<sup>2</sup> *Smolensk Branch of the Moscow Power Engineering Institute NRU, Smolensk*

\* *E-mail: kyacu@mail.ru*

### ABSTRACT

Results of experimental studying radiation spatial structure of atmosphere background non-uniformities and of an unmanned aerial vehicle being the detection object are presented. The question on a possibility of its detection using optoelectronic systems against the background of a cloudy field in the near IR wavelength range is also considered.

**Keywords:** optoelectronic systems, experimental studies, radiation spatial structure of atmosphere non-uniformities, IR spectral range

The last publications on study of atmosphere cloudy field radiation concern middle (3–5)  $\mu\text{m}$  and far infrared (8–13)  $\mu\text{m}$  wavelength (WL) [1–5]. In some foreign sources, data of space studies in IR spectrum on atmosphere composition and on weather forecasting are given in [6–10]. As to the data on atmospheres studies in the WL (1.5–2)  $\mu\text{m}$ , the publications are practically absent. And this fact interferes with solving a topical problem of detecting pilotless aircrafts (PLA) by means of passive optoelectronic systems.

In this regard, the authors have developed a technique of experimental studies of atmosphere radiation spatial structure non-uniformities in the WL (1.5–2)  $\mu\text{m}$  range with various cloud cover types. These studies were carried out in two stages:

- Record (measurement) of atmosphere radiance (R) fluctuation in Russia midland during winter and spring periods in the morning;

- The results processing in order to obtain statistical models describing principles of cloudy fields R fluctuation spatial structure.

To record R fluctuation of cloudy fields, a measurement computing system was developed, which basic element is a radiometer for the WL (1.5–2)  $\mu\text{m}$  spectral interval [11]. The radiometer contains as follows: a lens (Cassegrain's telescope), a rotated beam chopper driven by means of a step motor, an interference filter of (1.5–2)  $\mu\text{m}$  WL transmission band, a *PbS* photoresistor, and an electronic part (preamplifier, scale amplifier, low pass filter, analogue-digital converter, microcontroller and flash memory).

To evaluate parameters of the radiometer, calibration operations were made for the following purposes: to determine instant visual field, to plot calibration volt-thermal characteristics, to plot calibration volt-watt characteristics and to determine transmission coefficients of the radiometer channels, as well as to evaluate threshold sensitivity and expected measurement errors.

As a result of the performed operations, the following characteristics of the radiometer were determined: field width (20'  $\times$  20'), calibration volt-thermal characteristic; volt-watt characteristic, spectral characteristic in the WL (1.55–1.93)  $\mu\text{m}$ , transmission coefficient of the radiometer channel

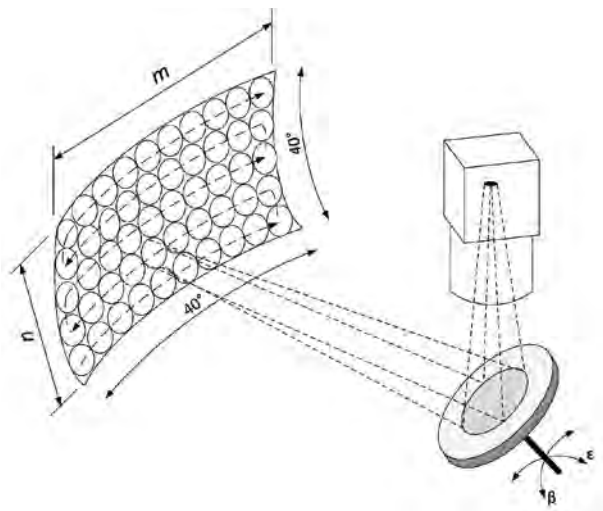


Fig. 1. A layout of scanning a cloudy field

( $5.324 \cdot 10^7$  V·cm<sup>2</sup>·strad/W), R threshold sensitivity ( $6.411 \cdot 10^{-10}$  W/(cm<sup>2</sup>·strad), R measurement error (10 %).

Control of step motors of the beam chopper and control of the scanning system mirror (Fig. 1) was implemented by a microcontroller. The commands came to the control unit via digital inputs (outputs) of the latter. Scanning sector of the selected atmospheric background (raster) fragment was provided within an interval to 40° in azimuth and within (10–50) ° in altitude angle. The scanning mirror provided pass of one frame line within the selected fragment of atmospheric background for 5 s. During this time, in every 30', 80 R values of this background were recorded. Upon completion of the frame line scanning, a signal came to the step motor, the mirror changed tilt angle by 1°, and scanning was repeated in the opposite direction. In a preset number of pitches (lines), step motors returned scanning mirror to the initial position, and record of the taken frame using a replaceable flash carrier was performed. Then the cycle was repeated, and the next frame was recorded.

A statistical processing of the measurement results of cloudy field R fluctuations was carried out upon termination of the measurement series, which consisted in creation of a pack of frames (raster), on average by 30 pieces. In total, nine types of cloudy fields under day time conditions were studied: cumulus (Cu) of 1–3 points (87 pieces); cumulus (Cu) of 4–6 points (91 pieces); cumulus (Cu) of 7–9 points (93 pieces); stratocumulus (Sc) (84 pieces); altocumulus (Ac) (73 pieces); cirrocumulus (Cc) (85 pieces); stratiform (Stf) (123 pieces), cirro-

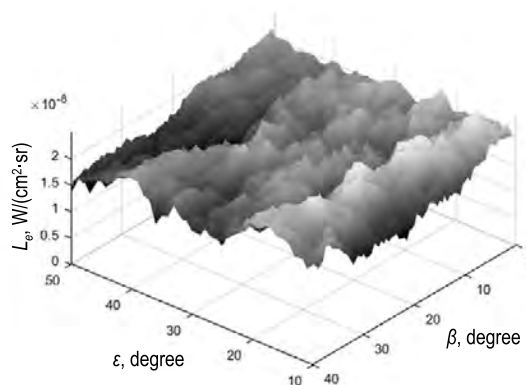


Fig. 2. A statistical model as a potential relief of radiance fluctuations average values distribution ( $L_e$ ) of 4–6 points cumulus cloud cover (Cu)

stratus (Cs) (118 pieces), cloudless sky (117 pieces). Totally 871 frames of cloudy fields were obtained.

Any such frame is a background image (BI) as a two-dimensional massif, which every element contains information on radiance level of the cloudy field in a selected direction. BI arrays can be a totality of lines and of columns (as matrices), an image in shades of grey or as a potential relief reflecting the spatial structure of atmosphere radiation non-uniformities.

Processing of the obtained BIs is carried out to obtain statistical models describing principles of R fluctuation of spatial structure of atmosphere cloudy fields. The BI processing results have shown that radiating non-uniformities of atmosphere cloudy fields are formed because of thermodynamic and turbulent atmospheric processes dependent on weather conditions. These non-uniformities have intrinsic angular dimensions and depend on cloud cover type, cloud amount, meteorological situation and day time.

After processing, the results are accumulated as packs of different type cloudy field BI frames and presented as matrices or as a potential relief of average values and dispersions (mean-square deviations) (RMSD) distribution. The obtained models can be considered to be statistical of the first type, which describe principles of spatial structure of atmosphere cloudy fields R fluctuations of the above named versions.

An analysis of the obtained statistical models of cloudy field radiance has shown that cumulus cloud cover (Cu) contains small-scale non-uniformities (Fig. 2). This can be explained by the fact that a cloudy Cu field has big vertical extent and in top

layers, ice crystals are contained, and in lower layers – water drops. As it is well-known [12], ice crystal reflection power in the WL (1.5–2)  $\mu\text{m}$  interval is higher than of water drops. Besides, a small increase of the R fluctuations average values and RMSD of a cloudy Cu field in the near-to-horizon area can be explained by influence of radiation reflection from Earth and from artefacts located on its surface.

Average values and dispersion (RMSD) of an alto-cumulus cloud cover (Ac) cloudy field R increase with increase of the altitude angle.

This result is explained by the fact that cloudy fields are formed at a big altitude and consist of ice crystals with a high reflection power in the WL (1.5–2)  $\mu\text{m}$  interval. And atmosphere influence in the near-to-horizon area increases because this area contains aerosols, which is absorbing a part of radiation.

In case of stratocumulus cloud cover (Sc), R average values and dispersion (RMSD) grow with increase of the altitude angle. This result is because of the fact that Sc type cloudy field is formed at a low height and mainly consists of water drops, which concentration increases in the near-to-horizon area as water drops to a great extent absorb WL radiation of the (1.5–2)  $\mu\text{m}$  interval [12].

During analysis of the obtained radiance statistical models for stratiform (St) cloud cover cloudy fields, it was revealed that average values and dispersion (RMSD) increase with increase of the altitude angle (Fig. 3). This is because St cloudy fields are formed at a low height and mainly consist of water drops, which concentration increases in the near-to-horizon area, and so they to a great extent absorb the considered type radiation [12].

Radiance average values and dispersions (RMSD) for stratiform cloudiness (Cs) cloudy fields are raise with increase of the altitude angle. This is because a Cs type cloudy field is formed at a big height and consists of ice crystals with high reflection power in the WL (1.5–2)  $\mu\text{m}$  interval. Reflection power decreases with reduction of altitude angle as distance between the measuring and computing system (MCS) and clouds increases; hence, radiation weakens because of absorption by atmosphere. A comparative low radiance value is explained by the fact that Cs type cloud structures are almost transparent.

Analysis results of the obtained statistical models of a clear sky hidden in morning haze have shown a high signal level. The reason of this is that

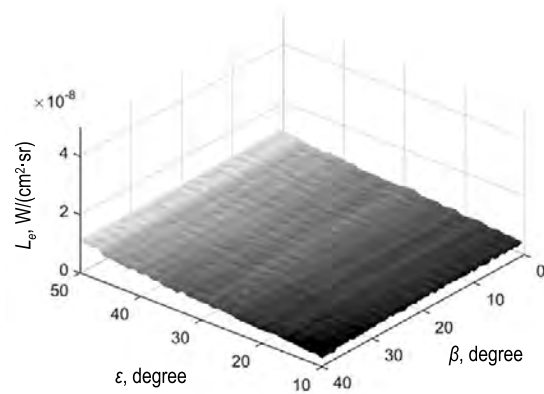


Fig. 3. A statistical model as a potential relief of radiance fluctuations average values distribution ( $L_e$ ) of stratiform cloud cover (St)

despite a large water drop quantity determining the haze composition, optical thickness of the latter is insufficient for strong radiation absorption as, for example, in the event of St type cloud cover. Increase of average values and of dispersion (RMSD) with increase of the altitude angle, is caused by reduction of optical thickness of the haze absorbing radiation.

Measured R values in the event the sky is clear, are at the level of the radiometer intrinsic noise. A low signal level is generally caused by almost full absorption of the measured radiation and weak reflection because of a low aerosol concentration in the near-to-horizon area and of ice particles in upper atmosphere.

Thus, an analysis of the first type statistical models, presented as dependences of average values and RMSD fluctuations of cloudy field radiance on the observation angle, showed that radiation intensity depends on cloud formation height, on cloud composition (ice crystals or water drops), and on particle concentration (ice crystals or water drops). If clouds are located highly, they mainly consist of ice crystals with a high reflecting power in the WL (1.5–2)  $\mu\text{m}$  interval and, therefore with increase of the altitude angle, increase of cloudy field R fluctuation average values and RMSD is observed. If clouds are located low, they mainly consist of water drops, which intensely absorb radiation, and so cloudy field R fluctuation average values and RMSD of are not too large. Besides, a small increase of big vertical extent cloudy fields R fluctuation average values and RMSD in the near-to-horizon area (Cu) is due to effect of radiation reflection from Earth and from artefacts (buil-

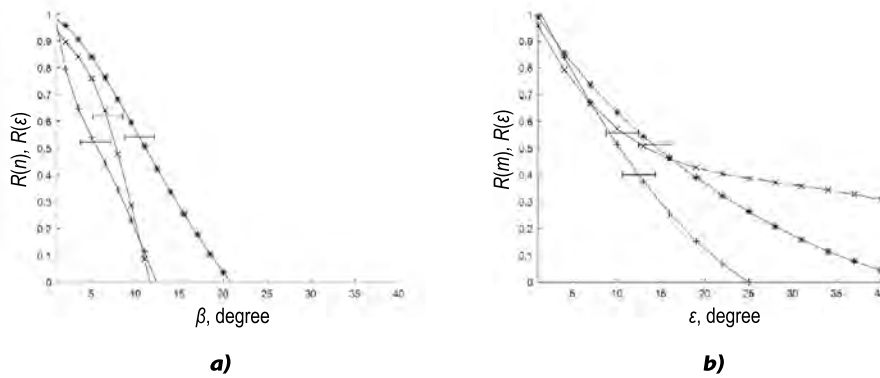


Fig. 4. Dependences of spatial correlation coefficient of a background image on angular shift linewise (a) and columnwise (b)

dings, trees, etc.) located on its surface. A dependence of cloudy field R fluctuation average values and RMSD on azimuth angles was observed with some types of cloud cover: cumulus (Cu), cumulonimbus (Cb), altocumulus (Ac), cirrocumulus (Cc), and cirrus (Ci).

Besides, an analysis of the obtained statistical models has shown that in depending on the non-uniformities size cloudy fields can be divided into two groups. The first one includes cloudy field types, which contain small-scale non-uniformities: cumulus (Cu), cumulonimbus (Cb), altocumulus (Ac), cirrocumulus (Cc) and cirrus (Ci). The second one includes large-scale non-uniformities, which size is more than dimensions of the obtained frames: stratiform (St), nimbostratus (Ns), stratocumulus (Sc), altostratus (As), and cirrostratus (Cs).

An analysis of the first type statistical models only allows understanding nature of the changes de-

pending on the observation altitude angle, which does not allow estimating angular dimensions of cloudy field non-uniformities.

To evaluate, how great these non-uniformities are, a correlation analysis of the first type models of different type cloudy field BI is necessary. The analysis should include calculation of mutual (spatial) correlation coefficients  $R$  and evaluation of their dependence on angular shift in two directions: linewise, and columnwise. The obtained dependences (Fig. 4) can be named statistical models of the second type reflecting principles of  $R$  fluctuation spatial structure. These dependences make it possible to estimate angular dimensions of cloudy field non-uniformities by the correlation radius value (angular values corresponding to the  $0.5 \cdot R$  level).

The fulfilled analysis has shown that cloudy fields of stratiform (St), stratocumulus (Sc), nimbostratus (Ns) and cirrostratus (Cs) of cloud cover types have large-scale non-uniformities: more than  $30^\circ$ . An analysis of spatial correlation relations for cumulus type of cloud cover (Cu) has shown that altitude angle non-uniformity values are approximately identical for all cloud amounts and are equal to  $7^\circ - 18^\circ$ . In the azimuth plane, non-uniformity values are similar  $5^\circ - 15^\circ$ .

A generalised analysis of all types of statistical models allowed revealing some features of cloudy field luminance characteristics in the WL (1.5–2)  $\mu\text{m}$  interval:

1. By statistical models, distributions of  $R$  fluctuations average values and RMSD of the first type cloudy fields have a trend of radiation intensity increase with increase of the observation altitude angle. Besides, they depend on formation height, cloud composition (ice crystals or water drops) and on particle concentration (ice crystals or water drops). They also allow dividing cloudy fields

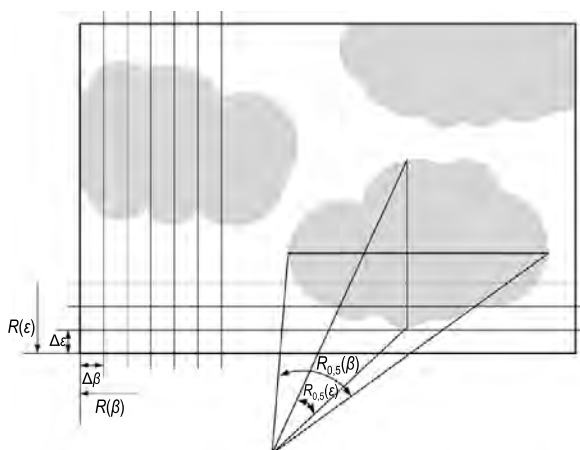


Fig. 5. An evaluation of cloudy field radiation spatial structure by correlation radii in horizontal and vertical directions, where  $R_{0.5}(\epsilon)$  and  $R_{0.5}(\beta)$  are correlation radii of spatial correlation functions computed between lines (columns) of a background image;  $\Delta\epsilon$  and  $\Delta\beta$  are angular discrete shifts when calculating spatial correlation functions for cumulus cloud cover (Cu)

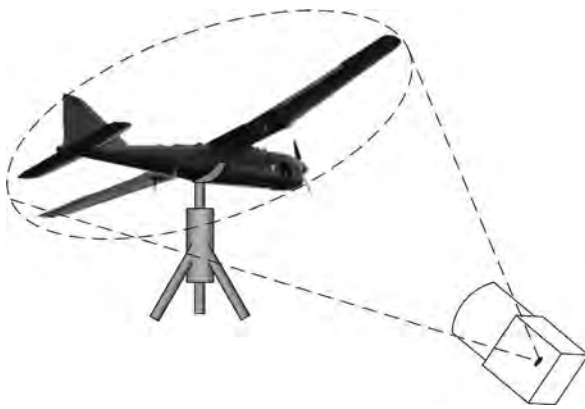


Fig. 6. The turning device with two freedom degrees

by their R into two types: with small-scale structure and with large-scale non-uniformities.

2. Spatial correlation functions of cloudy field R fluctuations have valuable coefficients of spatial correlation between BI neighbour lines ( $R_{n, n-1} \approx 0.9$ ) and columns ( $R_{m, m-1} \approx 0.9$ ). And therefore, as soon as a point object appears in a neighbour line (for example, a PLA image) radiating in a selected WL, one can expect a noticeable change of spatial correlation coefficient between neighbour lines, and then also between neighbour columns. A point object being PLA image is a little size object, which image fits well into  $N$  pixels ( $N \leq 5$ ) of the BI array [11].

Thus revelation of a line and a column, in which noticeable changes of spatial correlation coefficient are revealed, can serve to determine co-ordinates of a PLA within a BI cloudy field.

3. Angular dimensions of radiating non-uniformities of some type cloudy fields are limited by correlation radius values linewise and columnwise (Fig. 4). Therefore, dividing by width of PLA radiation spatial spectra and by extended radiating non-uniformities of cloudy fields is permissible.

4. Within BI segments with angular limitations equal to the correlation radiuses, spatial structure of cloudy field radiating non-uniformities linewise and columnwise is not subject to abrupt changes (Fig. 5) [12], i.e. can be considered to be uniform.

Thus, having obtained statistical models reflecting principles of a spatial structure (non-uniformity angular dimensions) of atmosphere cloudy field R fluctuations in the WL (1.5–2)  $\mu\text{m}$ , one can come to the second stage: study of PLA radiation energy characteristics.

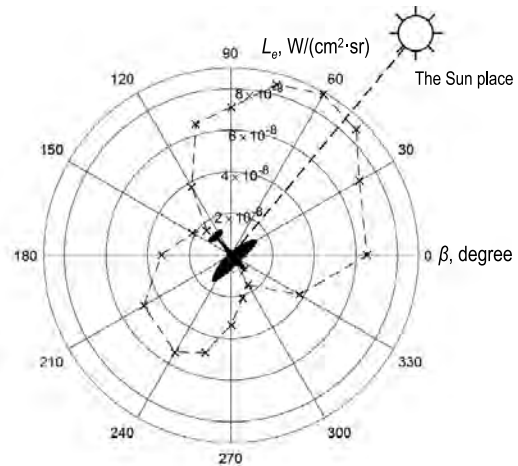


Fig. 7. A model as reflection indicatrix of a pilotless aircraft (altitude angle of its observation is  $10^\circ$ , position of the Sun is  $50^\circ$ )

There are several methods of experimental determination of PA radiance spatial distribution:

- Measurement method of PLA R while in flight. However, it is very complex to be implemented and requires a special equipment [13];
- Land-based method of measurement PLA R. It is measurement of PLA R in a preset WL using radiometric equipment moved around PLA.

To eliminate the main disadvantage of the latter (land-based) method, the PLA is fastened in a specially developed turning device with two freedom degrees (Fig. 6). This allows finding PLA reflection indicatrix (Fig. 7) not only in horizontal plane but also in case of changing its altitude angle position both in lower and in top hemispheres with switched-on, or switched off engine.

During the experiment studies, we have obtained PLA reflection indicatrix with one position of the Sun (azimuth  $50^\circ$ ) and with observation angle of  $10^\circ$ . Later on, the studies will be continued to obtain PA radiation statistical models as indicatrices for various positions of the Sun and different observation angles.

Taking into account properties of the statistical models describing features of R fluctuation spatial structure (non-uniformity angular dimensions) of cloudy fields in the WL (1.5–2)  $\mu\text{m}$  interval, it is revealed that for some cloud cover types, PLA detection is possible by using the direct threshold method.

But for some types of cloud cover (for example, Cu and Cb) this method is ineffective as R of some areas of cloudy field can be higher than of the searched point object.

Therefore, another approach should be used to solve the problem of the point object detection against the background of cloudy fields. This approach is that the searched point object is found by an analysis of cloudy field spatial structure features. This principle of obtaining information (background principle) makes it possible to solve the detection problem in an absolutely new way and to widen the traditional threshold detection method in cases when the latter is ineffective, namely when luminance contrast between the point object and cloudy field is slight, and object's image size does not exceed an element of the BI array [14].

When implementing the background principle, the detection system should be agreed with features of the atmosphere radiation spatial structure, which is much simpler, because background is an object slowly changing in space and in time.

## REFERENCES

1. Allenov A.M., Solovyov V.A. Correlation (spatial) relations between luminance fluctuations created by cloudy non-uniformities in the (8–13)  $\mu\text{m}$  interval / Proceedings of the IEM, 1995, Issue 25 (160): Atmosphere optics, pp. 3–15.
2. Allenov A.M., Solovyov V.A., Yakimenko I.V., etc. Studies of radiation of optical background in the (3–5)  $\mu\text{m}$  and (8–13)  $\mu\text{m}$  intervals / Proceedings of the IEM, 1996, Issue 26 (161), Physics of atmosphere, pp. 31–50.
3. Allenov A.M., Solovyov V.A., Yakimenko I.V. Structure of radiation of optical backgrounds in the (0.4–15)  $\mu\text{m}$  interval / Proceedings of the IEM, 1997, Issue 28 (163), Physics of atmosphere, pp. 3–41.
4. Allenov A.M., Ivanova N.P. Time changeability of the sky radiation spatial structure in the 8–13  $\mu\text{m}$  interval with cumulus cloud cover / The Optical journal, 2001, V. 68, #3, pp. 43–44.
5. Allenov M.I., Solovyov V.A., etc. Stochastic structure of cloud cover radiation / SPb.: Gidrometeoizdat, 2000, 175 p.
6. Knapp H.W. et al. Discriminating between water and ice clouds using near- infrared AVIRIS measurements // Summaries of the ninth JPL Aerborne Earth Science workshop, 2000, Feb 23–25, JPL.
7. Clough S.A., Shephard M.W., Mlawer E.J., Delamere J.S., Iacono M.J., Cady-Pereira K., Boukabara S., Brown P.D. Atmospheric radiation transfer modelling: a summary of the AER codes // Journal of Quantitative Spectroscopy and Radiation Transfer, 2005, Vol. 91, Issue 2, pp. 233–244.
8. Huang B., Mielikainen J., Oh H., Huang H.L.A. Development of a GPU-based high-performance radiation transfer model for the Infrared Atmospheric Sounding Interferometer (IASI) // Journal of Computational Physics, 2011, Vol. 230, Issue 6, pp. 2207–2221.
9. Lieven C., Hurtmans D., Clerbaux C., Hadji-Lazarro J., Ngadi Y., Coheur P.F. Retrieval of sulphur dioxide from the infrared atmospheric sounding interferometer (IASI) // Atmospheric Measurement Techniques, 2012, Vol. 5, Issue 3, pp. 581–594.
10. Chen X., Wei H., Xu Q. Infrared atmospheric transmittance calculation model // Infrared and Laser Engineering, 2011, Vol. 40, Issue 5.
11. Mishchenko A.M., Rachkovsky S.S., Smolin V.A., Yakimenko I.V. Experimental studies of spatial distribution of atmospheric background intrinsic radiation in the infrared wave length interval // Radio Engineering, 2017, #2, pp. 119–125.
12. Kriksunov L.Z. Handbook on foundations of infrared facilities. – Moscow: Sovetskoye Radio, 1978, 400 p.
13. V.A. Solovyov et al. Experimental determination of infrared radiation of planes while in flight, [a monograph], scientific-and-theoretical publishing / Ministry of defence of the Russian Federation, Smolensk: MA AAD of RF, 2009, 83 p.
14. Yakimenko I.V. Methods, models and facilities of detecting air targets against atmospheric background using wide-angle optoelectronic systems. The second revised edition, SPb.: Lan, 2014, 176 p.



**Anton M. Mishchenko,**

an officer of the Russian army, graduated from the MA AAD of RF AF in 2009. At present, he is Adjunct of the of Chair “Special radio engineering systems” of the MA AAD of RF AF, an author of five scientific works and of one software product for a computer, his scientific interest field is image digital processing, observation systems of various wavelength intervals and study of target intrinsic radiation in the optical interval

***Sergei S. Rachkovsky,***

an engineer, graduated from the Moscow Power Engineering Institute in 1988. At present, he is an engineer of the Chair “Computer engineering” of the MPEI NRU branch in Smolensk, an author of two scientific works. His scientific interest field is electronics and microprocessor facilities, study of intrinsic radiation of atmosphere and of the underlying surface in the optical interval, as well as development of measuring equipment and general purpose industrial grade installations

***Vladimir A. Smolin,***

an engineer, graduated from the Moscow Power Engineering Institute NRU in 2013. At present, he is a teaching assistant of the Chair “Electronics and Microprocessor Facilities of the Moscow Power Engineering Institute NRU branch in Smolensk. A postgraduate student of the MPEI NRU, an author of 40 scientific and educational-and-methodical works, as well as of two invention patents. His scientific interest field is digital image processing, electronics and microprocessor facilities, and study of atmosphere intrinsic radiation in the optical interval

***Igor V. Yakimenko,***

Dr. of Technical Science, Associate Professor, graduated from the Smolensk highest zenith rocket engineering school (1985) and the MA AAD of RF AF (2006). At present, he is the Head of the Chair “Electronics and Microprocessor Facilities of the MPEI NRU branch in Smolensk, an author of more than 200 scientific and educational-and-methodical works, 11 invention patents and 22 software products for computers. His scientific interest field is digital image processing, computer vision and systems of artificial vision, observation systems in different spectral intervals, study of intrinsic radiation of atmosphere and of the underlying surface and of intrinsic radiation of targets in the optical interval